

# Localized Active Space State Interaction: A Multireference Method For Chemical Insight

Riddhish Pandharkar,<sup>†,‡</sup> Matthew R. Hermes,<sup>†</sup> Christopher J. Cramer,<sup>¶</sup> and  
Laura Gagliardi<sup>\*,†,‡</sup>

<sup>†</sup>*Department of Chemistry, Pritzker School of Molecular Engineering, James Franck Institute,  
Chicago Center for Theoretical Chemistry, The University of Chicago, 5735 S Ellis Ave.,  
Chicago, IL 60637, United States*

<sup>‡</sup>*Argonne National Laboratory, Lemont, IL 60439, USA.*

<sup>¶</sup>*Underwriters Laboratories Inc., 333 Pfingsten Rd., Northbrook, IL 60062, United States*

E-mail: [lgagliardi@uchicago.edu](mailto:lgagliardi@uchicago.edu)

## Abstract

Multireference electronic structure methods, like the complete active space (CAS) self-consistent field model, have long been used to characterize chemically interesting processes. Important work has been done in recent years to develop modifications having lower computational cost than CAS, but typically these methods offer no more chemical insight than that from the CAS solution being approximated. In this paper, we present the localized active space - state interaction (LASSI) method that can be used not only to lower the intrinsic cost of the multireference calculation, but also to improve interpretability. The localized active space (LAS) approach utilizes the local nature of electron-electron correlation to express a composite wave function as an antisymmetrized product of unentangled wave functions in local active subspaces. LASSI then uses these LAS states as a basis from which to express complete molecular wave functions. This not only makes the molecular wave function more compact, but it also permits flexibility in choosing those states to include in the basis. Such selective inclusion of states translates to selective inclusion of specific types of interactions, thereby allowing a quantitative analysis of these interaction. We demonstrate the use of LASSI to study charge migration and spin-flip excitations in multireference organic molecules. We also compute the  $J$  coupling parameter for a bimetallic compound using various LAS bases to construct the Hamiltonian to provide insight into the coupling mechanism.

# 1 Introduction

Modeling chemically interesting phenomena like charge transfer, magnetic interactions, and excited states has long been an important objective for developments in electronic structure methods. Single-reference methods like density functional theory, popular for their ease of use, are poorly suited for systems with strong multireference character - i.e. significant non-dynamical correlation. Instead, multireference methods are required for such problems. A commonly used multireference method, the complete active space self-consistent field (CASSCF) model, provides a qualitatively correct description of the system that captures so-called static correlation.<sup>1</sup> This method requires the user to define the active space - a set of active orbitals and the number of electrons collectively occupying these orbitals. The CAS wave function is then expressed as a linear combination of all electronic configurations that can be obtained from all possible excitations of the active electrons in these active orbitals (within a given spatial and spin symmetry).

The exponentially growing cost of considering *all possible* configurations prevents CASSCF from being used for large systems with many strongly correlated electrons. Several cost-effective approximate methods have been developed based on the key insight that most of these configurations contribute very little to the wave function of the ground and low-lying excited states. Methods like the restricted (RAS)<sup>2,3</sup> or generalized active space (GAS)<sup>4</sup> models achieve this by limiting the number of electrons or holes in predefined subspaces. Alternatively, methods like density matrix renormalization group (DMRG)<sup>5</sup> iteratively optimize the matrix-product state representation of the wave function. Another popular approach, the selected configuration interaction (SCI)<sup>6-11</sup> model, usually starts with a small number of configurations and dynamically and iteratively expands the configuration space, either perturbatively (CIPSI<sup>12,13</sup>), adaptively (ASCI),<sup>14,15</sup> or stochastically (heat-bath CI<sup>16-18</sup> or FCI-QMC<sup>19,20</sup>).

We have previously proposed a form of multireference wave function that exploits the local nature of most electron correlation.<sup>21</sup> Named the localized active space (LAS) wave function, it decomposes a single active space into multiple subspaces that are localized on different parts of the molecule and can be assumed to be only weakly correlated to each other. The cost of computation

for a LAS wave function thus scales linearly with the number of fragments, which allows the study of large systems with multiple tractably small active subspaces.

The framework of using a basis of localized or fragment wave functions to obtain the overall wave function has been explored previously through various different approaches. In 1979, Liu and McLean proposed the interacting correlated fragment (ICF)<sup>22,23</sup> method that can incrementally introduce levels of electronic correlation between fragments in weakly interacting multireference systems. The active space decomposition (ASD) introduced by Parker and Shiozaki<sup>24-27</sup> in 2013 uses a similar approach to efficiently compute the CASSCF wave function using direct products of localized, orthogonal fragment states. Another recent approach, rank-one basis states by Nishio and Kurashige, also uses similar ideas and has been shown to work for large  $\pi$ -stacked systems.<sup>28,29</sup>

The LAS approach is equivalent to the cluster-based mean-field (cMF)<sup>30</sup> approach by Jimenez-Hoyos and Scuseria that expresses wave functions as a tensor-product state (TPS). The exact wave functions can be expressed in the basis of these correlated states using ansätze like couple cluster,<sup>31,32</sup> perturbation theory,<sup>33</sup> and many-body expansions.<sup>34</sup> The TPSCI algorithm by Abraham and Mayhall uses selected-CI methods to obtain the wave function in the basis of the TPS basis.<sup>35</sup>

While it is paramount that the cost of accurate multireference methods be lowered enough to be affordable for interesting systems, it is also important that we obtain substantial information *from* such calculations. For applications like computationally-guided materials design, or the study of site-site spin interactions in molecular magnets and environmental effects thereupon, calculations must not only give quantitatively accurate results, but to make progress they must also provide a better understanding of the system in terms of simpler chemical models used to interpret trends in properties and behavior. These models often use concepts that are easy to envision even if not accurate representations of underlying fundamental physics. For example, bonding in molecules is usually interpreted using concepts from valence bond theory (like bonding/anti-bonding orbitals, bond orders, etc.) even if the methods used for the calculations are not tied to such a representation. Similarly, reaction dynamics is often more easily interpreted by using diabatic surfaces. Another noteworthy example is the  $J$  coupling parameter that is used to explain spin-spin coupling

in magnets and the mechanisms by which that occurs: While a distinction between direct exchange and superexchange mechanisms may be useful for chemical interpretation, their effects are often difficult to quantify with electronic structure calculations. Instead, in many applications, the results from state-of-the-art electronic structure methods are fitted to these simple models to extract these parameters. In some simple cases, however, by comparing results from multiple cleverly selected active spaces one can obtain estimates of the contributions to these parameters.<sup>36,37</sup> There, however, is a need for a multireference method whose results are easy to interpret directly and is widely applicable to various problems.

As we continue to pursue multireference models that are widely applicable to various problems and whose results are easy to interpret, in this paper we explore the new state interaction (SI)-LASSCF formalism that builds on the LAS approach. The LASSI wave function is defined as a linear combination of multiple LAS states that form eigenfunctions of the molecular Hamiltonian. The choice of the LAS wave functions as a basis specifically allows us to selectively introduce coupling between the various subspaces. This framework fits well with the conceptual descriptions of many phenomena that are described by such interactions, like charge transfer and spin-spin coupling. We show that many important parameters can be calculated directly in this framework rather than extracting them by fitting CASSCF results to model Hamiltonians. Section 2 establishes the theoretical foundation and technical aspects of LASSI. Section 3 discusses the application performance of LASSI to intra-molecular charge transfer in an organic cation, the spin-spin coupling in a di-chromium complex, and the singlet-triplet gap in a growing series of conjugated polyenes.

## 2 Theory

### 2.1 LASSCF

The multireference LAS wave function decomposes the active space of the entire molecule into various subspaces. The wave function is then expressed as an antisymmetrized product of the full

configuration interaction (FCI) wave functions of the individual subspaces and the single determinantal wave function of the inactive space. The active subspaces are localized over the distinct user-defined fragments of the molecule while the inactive space is delocalized over the entire molecule. A general LAS wave function can be expressed as

$$|\text{LAS}\rangle = \left( \bigwedge_K |\Psi_{A_K}\rangle \right) \wedge |\Phi_U\rangle, \quad (1)$$

where  $\Psi_{A_K}$  is the many-body (generally FCI) wave function of the  $K^{\text{th}}$  localized subspace and  $\Phi_U$  is the single-determinantal wave function delocalized over the entire molecule. This is obtained by variationally optimizing the energy ( $E_{\text{LAS}}$ ) in equation 2

$$E_{\text{LAS}} = \langle \text{LAS} | \hat{H} | \text{LAS} \rangle \quad (2)$$

where  $\hat{H}$  is the molecular Hamiltonian.

In a typical LASSCF calculation, the user specifies the number of electrons ( $N$ ), magnetization ( $M_S$ ), spin ( $S$ ), and spatial symmetry point group ( $\Gamma$ ) for each subspace rather than for the entire molecule. A LAS state is uniquely defined by the set of these ‘local quantum numbers’ for all fragments  $\{(N_K, M_{S_K}, S_K, \Gamma_K) \forall K\}$ . Changing any one of these quantum numbers (within allowed values) creates different LAS states. In our previous work we have used this flexibility to change  $S$  and  $M_S$  for specific subspaces to model ground and excited spin states of the molecule.<sup>21,38</sup> For example, the ferromagnetic and anti-ferromagnetic coupling of locally high-spin (quintet)  $\text{Fe}^{\text{III}}$  centers were used to model the nonet and open-shell singlet states of the bimetallic  $[[\text{Fe}(\text{H}_2\text{O})_4]_2\text{bipyrimidine}]^{+4}$  molecule studied in references 21 and 39. In selected cases like the nonet, the LAS states can be accurate (if not exact) approximations. In other cases, however, a single LAS state can be only a crude approximation to the full molecular wave function. For instance, in the aforementioned case, the open-shell singlet is modeled using only one of many configurations that have an overall  $M_S = 0$ . As a consequence, these LAS wave functions are not eigenfunctions of the  $\hat{S}^2$  operator in cases where multiple active subspaces have non-singlet spins

that are not aligned to each other.<sup>21</sup> This requires the generation of symmetry adapted molecular wave functions as linear combinations of multiple LAS states.

Moreover, while the LAS approach has proven to be useful in studying localized excitations, it cannot be used directly to study delocalized excitations or strong inter-fragment coupling;<sup>21,38,39</sup> LASSCF accounts for the inter-fragment interaction only through a spin polarized mean-field. Further two-body interactions between the subspaces are often necessary for calculating quantities such as spin state ordering in strongly coupled multi-metallic compounds. In other words, the exact correlated wave functions for such systems cannot be expressed as a single tensor-product state, but instead need to be expanded as linear combinations of multiple states that couple to each other through such two-body interactions in the molecular Hamiltonian. In the limit of including all possible LAS states in the expansion, the resulting wave function accounts for the *exact* electron interaction. In many cases, however, even with a smaller number of LAS states, chosen based on chemical intuition, one can recover a significant part of this additional electron correlation.

## 2.2 Multiple LAS states

Similarly to state-average CASSCF, wave functions for multiple LAS states can be obtained in the same set of localized orbitals using the SA-LASSCF method by minimizing the energy expression:

$$E_{SA-LAS} = \sum_i w_i \langle \text{LAS}^{(i)} | \hat{H} | \text{LAS}^{(i)} \rangle, \quad (3)$$

where  $|\text{LAS}^{(i)}\rangle$  corresponds to the  $i^{\text{th}}$  LAS state with weight  $w_i$ . The SA-LASSCF wave functions are orthogonal, i.e. they diagonalize the LASSCF effective Hamiltonian, but can have off-diagonal elements (coupling) in the full-molecule Hamiltonian. In other words, these SA-LAS states are not eigenfunctions of the full-molecule Hamiltonian and suffer from the same problem highlighted in the previous section - namely the spin contamination and lack of inter-fragment coupling. These wave functions, however, are an excellent basis for the molecular wave function. The LAS state interaction (LASSI) method proposed in this work diagonalizes the molecular Hamiltonian con-

structed in terms of the SA-LAS states, to obtain molecular wave functions as linear combinations of LAS states (rather than that of n-particle excited states) as shown in equation 4.

$$|\text{LASSI}_i\rangle = \sum_j C_{ij} |\text{LAS}^{(j)}\rangle, \quad (4)$$

The LASSI wave functions are eigenfunctions of the Hamiltonian in the given LAS state basis:

$$\langle \text{LAS}^{(j)} | \hat{H} | \text{LASSI}_i \rangle = E_{\text{LASSI}}^{(i)} C_{ij}. \quad (5)$$

In general, these can be solutions to any arbitrary Hamiltonian constructed in the basis of SA-LAS states. In this study, we use only the standard electronic Hamiltonian of the entire molecule, but in principle any other electronic structure method can be used to obtain this Hamiltonian (effective potentials, PDFT, etc.) and effects like spin-orbit coupling can also be included to couple the LAS states. The LASSI is a one shot diagonalization of the full-molecule Hamiltonian in a basis much smaller than that of all configurations within the complete active space. Similar to methods like RAS/GAS-SCF, which approach the exact solution (CASSCF) as we increase the number of configuration state functions (CSF), the LASSI wave function also approaches the exact solution in the limit of including all possible LAS states in the LASSI. However, a LAS state typically includes more correlation than a CSF and thus the CI vector of the exact solution can be significantly more compact in this basis. This means, importantly, that as we expand the basis of the wave function we can account for more correlation faster when expanding in the LAS basis than expanding in the CSF basis.

While the primary motivation of this method is the restoration of inter-fragment coupling, one can think of LASSI also in the context of diabaticization. This perspective is particularly helpful when computing potential energy surfaces for chemical reactions. The LAS states do not change chemical character imposed on them along a reaction coordinates and thus are analogous to diabatic states, while the LASSI wave functions are solutions of the Hamiltonian and are thus the adiabatic states. The LASSI procedure is simply a transformation of the LAS states (model di-

abatic states) - that are comparatively straight forward to compute - to obtain the LASSI states that correspond to the uniquely defined eigenfunctions of the molecular Hamiltonian and conserve symmetries across the potential energy surface.

### 2.3 Selecting the LAS states for state interaction

For most chemical systems, the choice of the LAS states is non-trivial and a robust protocol that automates this choice can reduce dependence on the experience of the practitioner. We outline here a scheme that incrementally includes different types of states to systematically improve the quality of the solution depending on the problem in hand.<sup>40,41</sup>

Each LAS calculation is initialized with a certain number of active electrons occupying the active orbitals in each subspace. Using these as a reference we can allow up to  $n$  excitation from one fragment to the other to obtain charge-transfer (CT) states. All possible states that can be reached by having up to  $n$  CT excitations are considered - including states with multiple concerted excitations - in order to achieve size consistency. For example for  $n = 1$  (single charge transfer excitations) we also include states that have concerted single excitations in multiple different pairs of subspaces. For any LAS state, the net difference in the active electrons belonging to a subspace in that state with respect to the reference LAS state is termed as the charge on the subspace. This charge defines only the total number of electrons in each active subspace. This can, in principle, allow a large number of spin states. Some of these spin states may be very high in energy and may not be of particular interest. Depending on the chemical characteristics of the subspace the user has an option to limit the spin ( $S$ ) of each fragment to a certain range. For instance, in a subspace of 6 electrons in 6 orbitals localized on a phenyl ring, one might choose to only include singlet and triplet states and exclude the quintet and septet states that are technically possible but unlikely to contribute to the wave function. The spin projection quantum number ( $M_s$ ) is the other quantum number that uniquely characterizes a LAS state. All  $M_s$  values ranging from  $-S$  to  $S$  for each spin for each subspace are included in the SI Hamiltonian. While it is possible to include only a subset of the  $M_s$  values in the state average manifold, we do not recommend this choice for it might result



in the LASSI states not being proper spin eigenfunctions.

The states included in the SI Hamiltonian are not necessarily low-lying states. In some cases, the inclusion of high-energy states (like a charge-separated state or an excited spin state) in the SI Hamiltonian may be necessary if they couple strongly with the ground or low-lying excited states. It can, however, be detrimental to include them in the state-average manifold while optimizing the orbitals. Since the orbitals in SA-LAS are optimized to minimize a collective energy, the description of the ground state (or the particular state of interest) is compromised by these states. To avoid this, we can exclude the high energy states from the orbital optimization procedure; i.e., by setting their weights ( $w_i$ ) in equation 3 to zero. This is similar to the strategy often used in SA-CASSCF - where the orbitals optimized from a calculation with a fewer states are used to perform a CASCI calculation for a larger number of roots. Specific details of the state selection schemes used in each application are provided in the respective sections. It must be noted that in the limiting case of approaching CASSCF - i.e. considering all possible CT excitations and spins - the method also scales exponentially with respect to the size of the active space like CASSCF. Although reducing the size (and thus increasing the number of fragments) always reduces the cost of the computation for a single-state LASSCF calculation, that is not the case for LASSI since the number of states to be considered for SI increases with the number of fragments. Thus it is important to strike a balance in the fragmentation schemes used in LASSI such that the subspaces are not too large for the FCI solver in the subspace, but also not so numerous that the exponential scaling of the size of the SI Hamiltonian can be handled.

### 3 Applications and Discussion

We demonstrate the scope and performance of LASSI in three different applications shown in figure 1. All calculation were performed using the mrh<sup>40</sup> and PySCF<sup>42</sup> packages. For all the systems studied the def2-svp basis was used for the C,N,O,H while def2-tzvp basis was used for the Cr atoms in system 2. Details about choice of active space and state averaging are discussed in

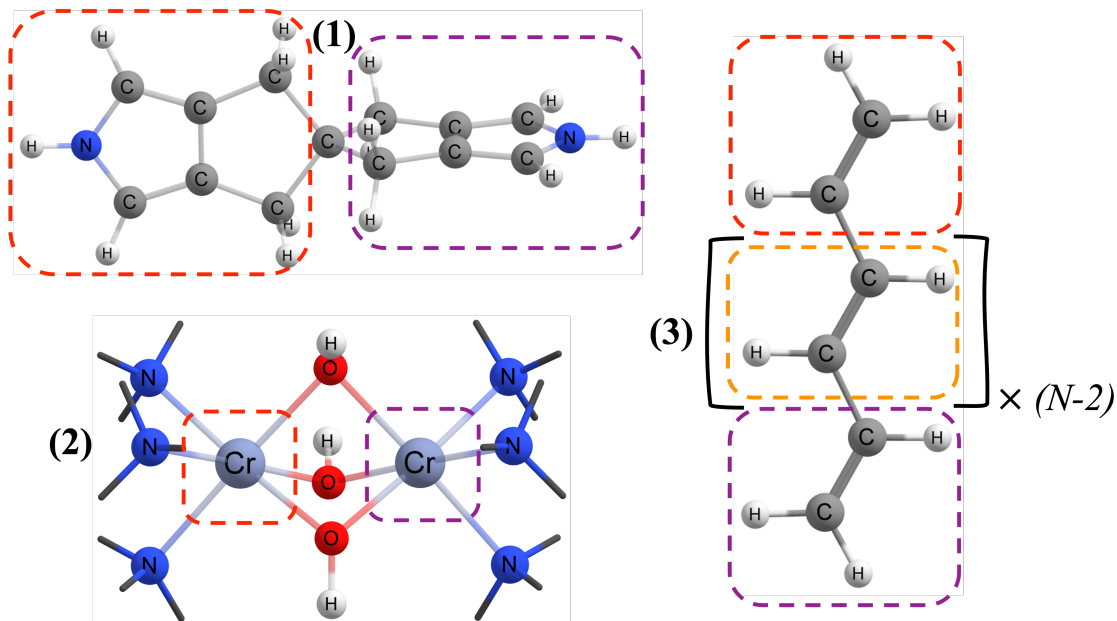


Figure 1: The systems studied: (1) 2,2',6,6'-tetrahydro-4H,4'H-5,5'-spiro[cyclopenta[c]pyrrole]<sup>+</sup>, (2) [Cr<sub>2</sub>(OH)<sub>3</sub>(NH<sub>3</sub>)<sub>6</sub>]<sup>3+</sup> and (3) *trans*-polyenes C<sub>2N</sub>H<sub>2N+2</sub>. The fragmentation schemes for their active spaces are shown by dotted lines.

the respective sections.

### 3.1 Charge transfer

Charge transfer plays an important role in many chemical and biological processes.<sup>43–48</sup> The process of charge transfer is often modeled with two approaches: either by constructing the Hamiltonian in a basis of diabatic, charge-separated states and then diagonalizing it to get the adiabatic states or to directly obtain the adiabatic ground and excited states (with an electronic structure method of choice) to begin with and then assign charge-transfer character to them. While the later approach is more popular because of its generality, the former is often used to interpret results and understand mechanisms of charge transfer. A key challenge for the former approach, however, is to obtain this chemically intuitive diabatic basis in an efficient way. Approaches such as valence-bond theory and constrained density functional theory have been used previously for this purpose. In this section we highlight that LAS states can be an excellent choice for the diabatic basis, especially when the donor and acceptor species involved are multireference in nature. Moreover, the

adiabatic surfaces that can be easily obtained from these LAS states after state interaction, are just as good as the surfaces obtained from more expensive methods like CASSCF.

The 2,2',6,6'-tetrahydro-4H,4'H-5,5'-spirobi[cyclopenta[c]pyrrole] cation, system **1**, is often used as a prototype to study the performance of electronic structure methods describing charge transfer. The compound consists of two partially saturated cyclopenta[c]pyrrole rings that are perpendicular to one another. While the neutral compound is highly symmetric with a  $D_{2d}$  point group, the cation has most of the positive charge localized on one of the rings thus breaking the symmetry in its equilibrium structure. Since the two states of charge being localized on the two rings respectively are non-degenerate at the equilibrium geometry, there exists a finite barrier for this charge migration to happen. We study the potential energy surface (fig 3) for this charge migration using CASSCF, LASSCF and LASSI with an active space containing the 11  $\pi$  electrons in the 10  $\pi$  orbitals. The LAS subspaces are composed of the 6  $\pi$  orbitals localized on each ring with 5 electrons in one and 6 in the other. The other charge separated state is obtained when the number of electrons in each subspace is interchanged. The geometries along the potential energy surface were obtained from reference 49 that uses a unitless progress variable,  $\xi$ , to linearly parameterize the Cartesian coordinates along the reaction pathway. In this work, we consider  $\xi$  from -0.8 to +0.8 where -0.5 and 0.5 are the equilibrium structures corresponding to the charge being localized on the left and right side respectively. The potential energy curves for the two LASSCF states

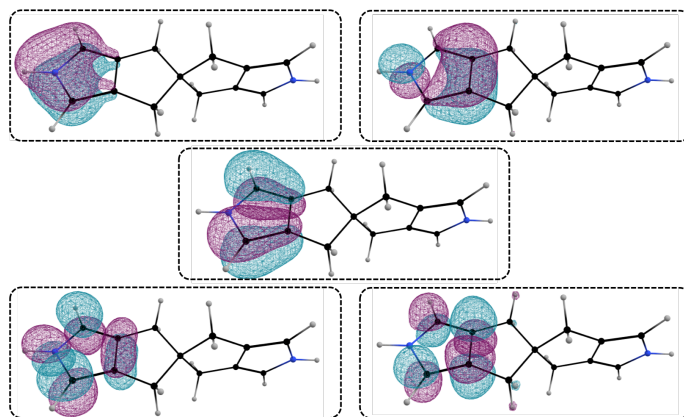


Figure 2: Active orbitals for the subspace localized on one of the cyclopenta-[c]pyrrole in system **1**. The other subspace included equivalent orbitals on the other cyclopenta-[c]pyrrole.

show a crossing at  $\xi = 0$ . This is expected because the LAS states do not interact with each other. We consider only the LAS states corresponding to one subspace in a doublet spin-state (for the ring with the positive charge) and the other with a singlet spin in the LASSI calculation. Excited states with other spin-states or with more than one electron migrating between the subspaces are ignored. The LASSI energies are identical to the larger CASSCF, showing that only these two states dominate the coupling term.

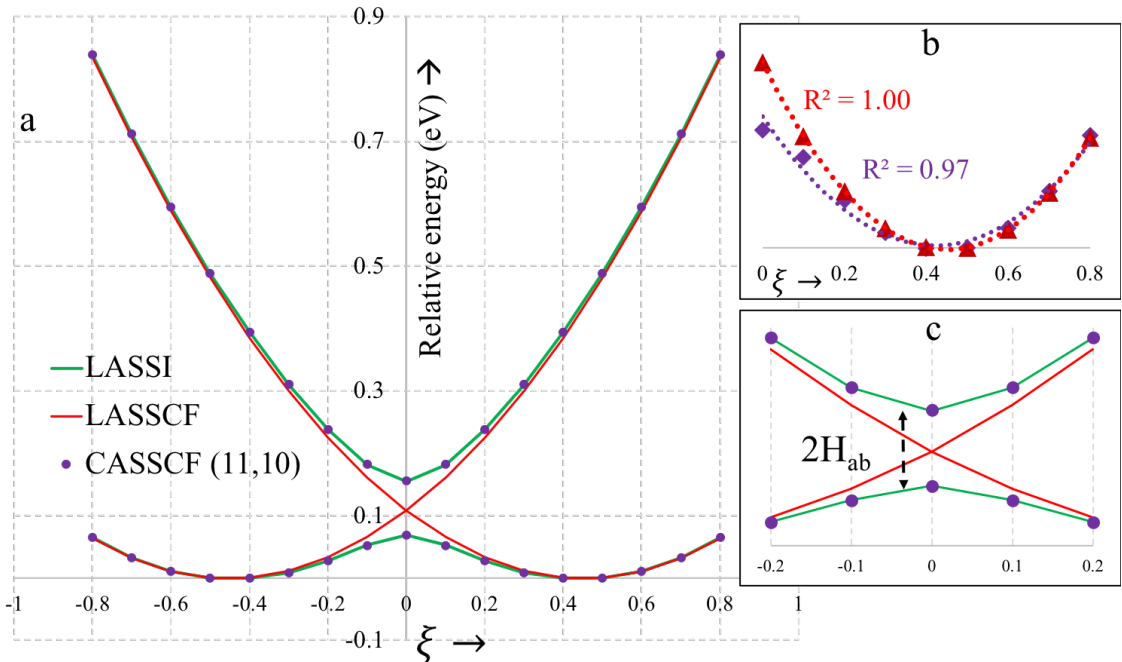


Figure 3: (a) Potential energy surface for the charge migration in **1** obtained from LASSCF, LASSI and CASSCF as a function of the dimensionless reaction coordinate ( $\xi$ ). (b) The fitted quadratic curves (dotted lines) for the LASSCF and CASSCF energies along with their  $R^2$  values. (c) a magnified plot of the PES on the left around the crossing point along with the gap indicating  $H_{ab}$ .

The Hamiltonian matrix element  $H_{ab}$  that couples the diabatic states is an important quantity that is used to classify and study charge transfer. This quantity is not explicitly computed using methods like CASSCF. The gap at the avoided crossing is often used to estimate  $H_{ab}$ . The gap with CASSCF is 0.16 eV. Since this is equal to  $2 \times H_{ab}$  for a two-state model (fig. 3c) the coupling element ( $H_{ab}$ ) is 0.08 eV. While LASSI reproduces this energy surfaces well and also gives a  $H_{ab}$  of 0.075 eV, LASSI arrives at this result in a different way. It explicitly calculates this coupling

matrix in the basis of the LAS states and then mixes them to give the gap. This shows that the LAS states are good candidates for the diabatic states that provide interpretability as well as good accuracy. Another parameter that is needed for analyzing CT is  $\lambda$ , the quadratic coefficient of the parabola of the diabatic curve that dictates its stiffness. The  $\lambda$  value along with the  $H_{ab}$  is used to calculate the rates for charge transfer. As seen in figure 3b, the LASSCF curves fit perfectly to a parabola and give a  $\lambda$  of 0.53 eV. If however, one were to extract this number from the adiabatic CASSCF curves (or even LASSI) it would have some anharmonicity and give a  $\lambda$  of 0.42 eV. While this estimate for CASSCF can be made better by performing a finer scan in the region close to the equilibrium geometry, no such calculations are required for LASSCF. Any three points along the scan give similar value for  $\lambda$ .

The method of finding the CT state in CASSCF also involves significant trial-and-error in choosing sufficiently many excited states in the averaging manifold. Importantly, since we can selectively include only charge-states in the LASSI Hamiltonian, this approach does not suffer from the need to include all excited states lower than the CT states in the state-averaging manifold that might compromise the description of the CT states. This becomes helpful when studying systems like DNA base pairs and mixed-valency metal complexes that can have multiple excited states lower than the CT states.

## 3.2 A bimetallic compound

Multi-metallic compounds are interesting for many applications.<sup>50-52</sup> The coupling between their spin centers can be modeled using the effective Hamiltonian from the Heisenberg-Dirac-Van Vleck model.<sup>53-55</sup> This invokes a magnetic coupling parameter,  $J_{ab}$ , that couples the spins localized on the two centers  $a$  and  $b$  and characterizes the type and extent of coupling between them. By convention, a negative  $J$  indicates antiferromagnetic coupling and a positive  $J$  indicates a ferromagnetic one. The higher the magnitude of  $J$ , the stronger the coupling between the spin centers. Most computational methods calculate  $J$  using the Yamaguchi formula (6), that expresses it in terms of the energy difference between the high-spin and low-spin states:

$$J_{ab} = \frac{E_{HS} - E_{LS}}{\langle \hat{S}^2 \rangle_{LS} - \langle \hat{S}^2 \rangle_{HS}}, \quad (6)$$

To avoid the spin-symmetry breaking that occurs in DFT (and other single-determinant methods) and instead compute  $E_{LS}$  directly, multireference methods are needed. For quantitatively accurate spin gaps, however, large active spaces are required to model the interactions in such compounds. This becomes prohibitively costly in the presence of more than two metal centers. The coupling between the multiple metal centers is affected by many factors. Some of these are understood through different conceptual mechanisms like direct exchange/through-space coupling or super-exchange, etc. Most multireference methods, even with approximate solvers that allow us to go to larger systems, do not offer easily interpretable quantitative insights into the contributions of these mechanisms. By contrast, LASSI can be very useful.

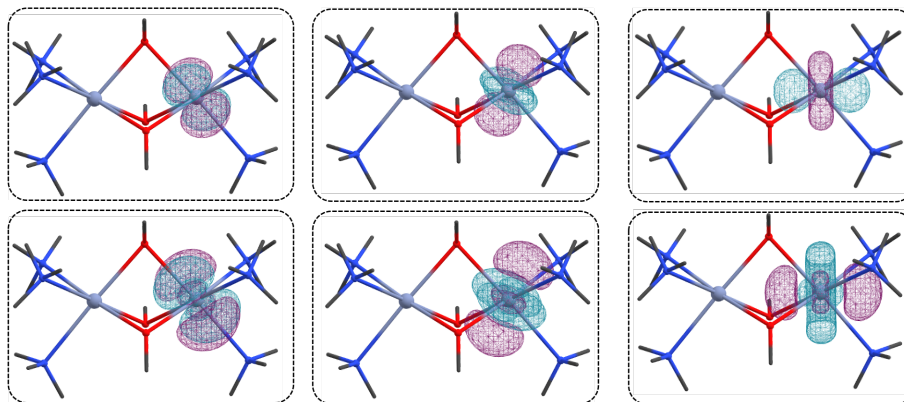


Figure 4: Active orbitals for the subspace localized on one Cr ion.

We consider here the coupling between the two high spin metal centers in **2**. This compound is a model for a tris-( $\mu$ -hydroxo)-bridged chromium compound studied experimentally and theoretically.<sup>37,56–59</sup> The more complex actual ligands were truncated to ammonia molecules having appropriately positioned nitrogen atoms. The two chromium [III] ions have three unpaired electrons each. The active space we consider for a full-molecule CASSCF calculation is that of 6 electrons in 12 orbitals that corresponds to all the singly occupied 3d orbitals on the Cr centers and

their corresponding 4d (correlation pair) orbitals (see Fig. 4). The CASSCF (6,12) calculations predict a  $J_{ab}$  of  $-16.7 \text{ cm}^{-1}$ . This indicates that the compound is anti-ferromagnetic. The spin ladder for CASSCF in figure 5 shows that the singlet ( $S = 0$ ) state is about  $200 \text{ cm}^{-1}$  lower than the septet ( $S = 3$ ) state. The experimental value for the J-coupling constant is  $-66 \text{ cm}^{-1}$ . Previous investigations have shown that a quantitative prediction of the constant will not only require a much larger active space but also needs to include post-MCSCF methods to include more dynamic correlation.<sup>37,60</sup> The purpose of this study is not to reproduce the experimental value (and, indeed, it is likely that ammonia ligands in place of the actual ones would affect that value), but to analyze how LASSI can approach the CASSCF limit.

The overall coupling captured in CASSCF can be primarily associated with two conceptual mechanisms: ‘direct’ exchange and ‘kinetic’ exchange.<sup>61,62</sup> Note that any superexchange mechanism is not captured here since we do not include any linker orbitals in the active space. The ‘direct’ exchange contribution arises from coupling elements associated with direct exchange integrals involving one orbital localized on one spin center and the second on the other spin center. Since these integrals are always positive they contribute to a positive value of  $J$ , i.e., ‘direct’ exchange favors the high-spin state. The kinetic exchange, however, accounts for the coupling of the ground state with configurations involving excitations from one spin center to the other (ionic configurations). Its magnitude depends on coupling between neutral and ionic configurations (a hopping integral). This coupling favors an antiferromagnetic ground state and contributes to the lowering of  $J$ . Thus, the overall sign of  $J$  is determined by how large the kinetic exchange terms are relative to direct exchange. These concepts and relations are derived and explained for the case of two unpaired electrons in two orbitals in references 62 and 61. The negative sign of the CASSCF  $J$  means that the compound is antiferromagnetic and thus that the kinetic exchange dominates the coupling. There is, however, no simple way to quantify this contribution to the CASSCF wave function. This is where LASSI offers a particular advantage - by selectively including the states corresponding to each of the mechanisms in the LASSI basis we can ‘switch-on’ or ‘switch-off’ different mechanisms of coupling between the fragments.

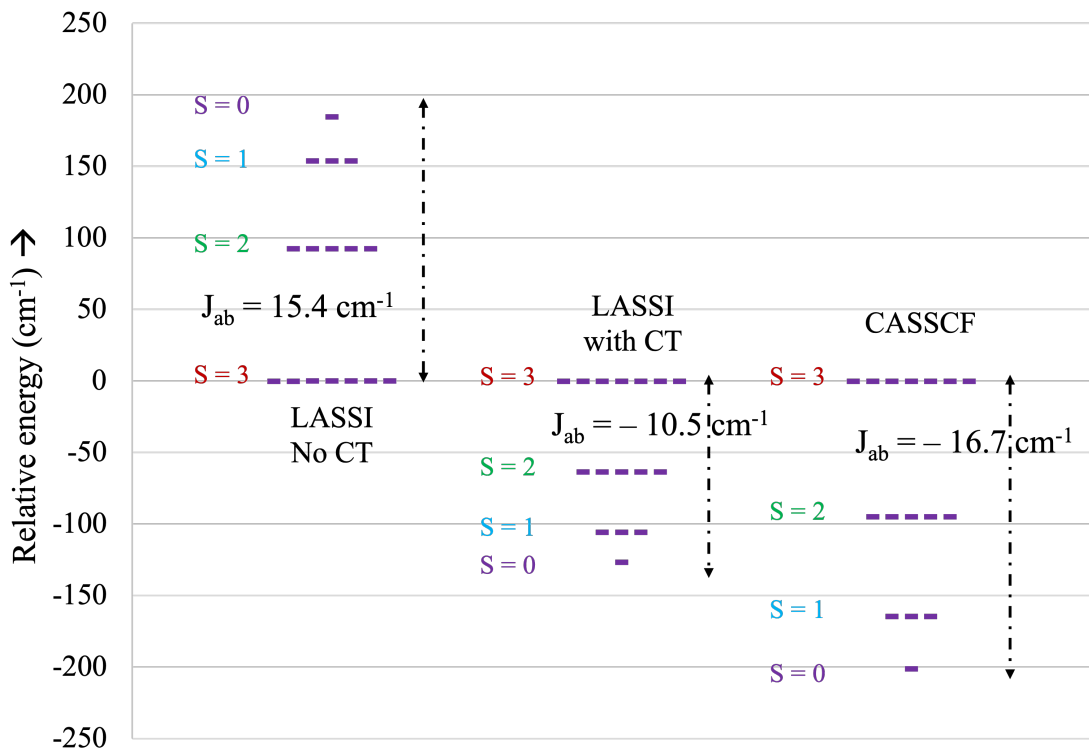


Figure 5: Spin ladder for the bimetallic compound calculated using various methods relative to the septet energies for the respective method. The number of purple dashes indicates the multiplicity of the state. The  $J$  value calculated using the singlet-septet gap is shown for each ladder.

We perform LASSI calculations where we divide the (6,12) active space into two subspaces of (3,6) localized on each Cr atom (see Fig. 4). If the SI Hamiltonian is constructed only in the space of the neutral states, the only off-diagonal terms are the direct exchange terms. The  $J$  value is positive, as it must be, and significantly so at  $15.4 \text{ cm}^{-1}$ . As seen in figure 5, the singlet ( $S = 0$ ) state is about  $185 \text{ cm}^{-1}$  higher than the septet ( $S = 3$ ) state. When we include the states with inter-fragment electron hopping, however, the spin state ordering is correct and the  $J$  is lowered to  $-10.5 \text{ cm}^{-1}$ . This means that the kinetic exchange terms, that are now introduced in the SI Hamiltonian, contribute about  $-25 \text{ cm}^{-1}$ . In such a way we were able to quantify the two contributions separately. Figure 5 shows the qualitative similarity in the spin ladder predicted by CASSCF and LASSI with CT states. By including the CT states in the SI Hamiltonian we have not only computed the correct spin state ordering but have achieved agreement with the full CASSCF  $J$  value to within  $6 \text{ cm}^{-1}$ . This calculation is, in principle, cheaper than CASSCF (and will become increasingly so with



possibly more centers and/or more active electrons/orbitals on each center), and at the same time provides more information and insight into the system. Of course, the LASSI  $J$  value is *not* the same as the CASSCF value because CASSCF includes more configurations than those employed for the LASSI basis, but a systematic approach to *adding* those configurations could be undertaken where deemed useful.

### 3.3 Delocalized spin states: Case study in polyenes

Methods to accurately predict singlet-triplet (S-T) gaps for long conjugated compounds are of interest for a wide range of applications.<sup>63–68</sup> A chemically intuitive fragmentation scheme, with a set of  $\pi$  and  $\pi^*$  orbitals localized on smaller units like  $C_2H_2$  or  $C_4H_4$ , would in principle provide a significant advantage in terms of numbers of configurations needed with increasing size of the molecule. State-specific LASSCF with such a fragmentation describes reasonably well the ground-state singlet which is dominated by the closed shell configuration. However, it is not suited for calculating the S-T gaps as it is not able to capture the delocalized nature of the unpaired electrons of the triplet. Since only one of the active subspaces can have a triplet spin, the two unpaired electrons are perforce localized only on that fragment. This is a nonphysical description since the true triplet has the two electrons delocalized (to varying degree) over the entire molecule. This is a typical situation where LASSI is superior to LASSCF and more affordable than CASSCF.

Table 1: Singlet-triplet gaps (eV) from CASSCF, LASSCF, and the various schemes of LASSI

$n$	CASSCF	Subspace decomposition	LASSCF	LASSI		Experiment
				no CT	with CT	
2	3.42	$(4, 4) \rightarrow \wedge_2(2, 2)$	4.29	4.62	3.43	3.22 <sup>69</sup>
3	2.80	$(6, 6) \rightarrow \wedge_3(2, 2)$	4.10	4.79	2.86	2.61 <sup>70</sup>
4	2.39	$(8, 8) \rightarrow \wedge_4(2, 2)$	4.01	4.88	2.48	2.10
		$(8, 8) \rightarrow \wedge_2(4, 4)$	3.30	3.41	2.66	
8	–	$(16, 16) \rightarrow \wedge_4(4, 4)$	3.16	3.53	2.10	–
12	–	$(24, 24) \rightarrow \wedge_4(6, 6)$	2.62	2.75	1.98	–

Table 1 shows the singlet-triplet gaps computed with CASSCF, LASSCF, and LASSI for five linear polyenes  $C_{2n}H_{2n+2}$  with  $n = 2, 3, 4, 8,$  and  $12$ . The complete active space of size  $(2n, 2n)$

composed of the  $\pi$  and  $\pi^*$  orbitals is divided into  $n$  subspaces of (2,2) for  $n=2, 3$ , and 4 ( $\wedge_n(2, 2)$  fragmentation) and into  $n/2$  subspaces of (4,4) for  $n = 4$ , and 8 ( $\wedge_{n/2}(4, 4)$  fragmentation), and finally 4 subspaces of (6,6) for  $n = 12$ . Two schemes have been used to construct the LASSI Hamiltonian: one where only neutral configurations with singlets and triplet spins are used and the other where charge-transfer configurations with one electron hopping were also included. The orbitals for LASSI were obtained by state-averaging over the singlet ground state and states with up to two triplet fragments. This truncation of the space was used only for the orbital optimization for computational efficiency, while all possible states were considered when constructing the LASSI Hamiltonian.

We observe that the CASSCF gap reduces with increasing length of the conjugated chain. The LASSCF with the triplet localised on one fragment not only gives the wrong quantitative gap but also shows minimal change with increasing chain size. The gap stays around the same as that of a single ethylene molecule for the  $\wedge_n(2, 2)$  fragmentation.

In the LASSI calculations, the cases without the charge transfer (hopping) states included in the SI Hamiltonian show poor performance. However, LASSI captures the trend of a decreasing gap when we include the charge transfer states. Note that this improved accuracy of the singlet-triplet gaps derives from the treatment of the two spin states at equal footing and *not* because the LASSI states (and corresponding electronic energies) are necessarily individually close to their CASSCF equivalents.

As expected, using the larger (4,4) subspaces provides LASSCF (and LASSI without charge-transfer) singlet-triplet gaps having the essentially constant value associated with butadiene, and again, including charge-transfer states in LASSI significantly reduces that gap (although there is not an experimental value against which to compare for  $n = 8$ ). This trend continues for  $n=12$ , where the larger (6,6) subspaces permit many intra-subspace charge-transfer interactions to be included in the LASSCF itself so that those associated only with the LASSI calculation have smaller (but still important) quantitative impact.

## 4 Conclusions

LASSI is an extension of the LASSCF method(s) that overcomes some of the challenges associated with LASSCF by constructing eigenfunctions of the molecular Hamiltonian in a basis of LAS states. LASSI not only allows us to systematically improve the wave function - formally approaching the CASSCF limit - but it also offers opportunities to better provide chemical interpretations of results by considering alternative LASSI schemes. The method's control over the natures of interactions within and between fragments can be leveraged to study phenomena like charge transfer and spin coupling in detail. In future work, we anticipate the productive application of this method to larger systems to study phenomena like intravalent charge transfer in organometallic compounds and superexchange mediated J-coupling in multi-metallic compounds. Further improvements in scaling may be achieved by using other approaches to couple the subspaces like DMRG or (unitary) coupled cluster. In addition, more quantitative predictions may be realized by capturing additional electron correlation using methods like perturbation theory or pair-density functional theory.

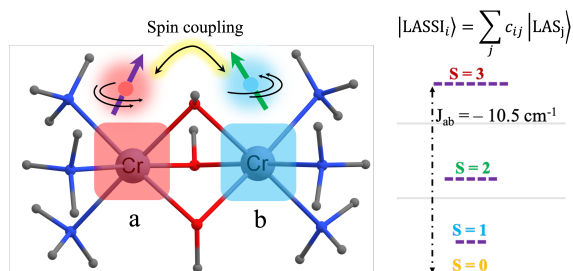
## Acknowledgement

This material is based upon work supported by the U.S. Department of Energy, Office of Science, National Quantum Information Science Research Centers. The computational resources for this project were provided by the University of Chicago Research Computing Center (RCC).

## Supporting Information Available

Absolute electronic energies, and equilibrium molecular geometry Cartesian coordinates are provided.

## ToC Graphic



## References

- (1) Roos, B. O.; Taylor, P. R.; Siegbahn, P. E. M. A Complete Active Space SCF Method (CASSCF) Using a Density Matrix Formulated Super-CI Approach. *Chem. Phys.* **1980**, *48*, 157.
- (2) Malmqvist, P. Å.; Rendell, A.; Roos, B. O. The restricted active space self-consistent-field method, implemented with a split graph unitary group approach. *J. Phys. Chem.* **1990**, *94*, 5477–5482.
- (3) Olsen, J.; Roos, B. O.; Jørgensen, P.; Jensen, H. J. A. Determinant based configuration interaction algorithms for complete and restricted configuration interaction spaces. *J. Chem. Phys.* **1988**, *89*, 2185–2192.
- (4) Ma, D.; Li Manni, G.; Gagliardi, L. The generalized active space concept in multiconfigurational self-consistent field methods. *J. Chem. Phys.* **2011**, *135*, 044128.
- (5) Chan, G. K.-L.; Head-Gordon, M. Highly correlated calculations with a polynomial cost algorithm: A study of the density matrix renormalization group. *J. Chem. Phys.* **2002**, *116*, 4462–4476.

- (6) Bender, C. F.; Davidson, E. R. Studies in Configuration Interaction: The First-Row Diatomic Hydrides. *Phys. Rev.* **1969**, *183*, 23.
- (7) Whitten, J. L.; Hackmeyer, M. Configuration Interaction Studies of Ground and Excited States of Polyatomic Molecules. I. The CI Formulation and Studies of Formaldehyde. *J. Chem. Phys.* **1969**, *51*, 5584.
- (8) Tubman, N. M.; Lee, J.; Takeshita, T. Y.; Head-Gordon, M.; Whaley, K. B. A deterministic alternative to the full configuration interaction quantum Monte Carlo method. *J. Chem. Phys.* **2016**, *145*, 44112.
- (9) Schriber, J. B.; Evangelista, F. A. Communication: An adaptive configuration interaction approach for strongly correlated electrons with tunable accuracy. *J. Chem. Phys.* **2016**, *144*, 161106.
- (10) Liu, W.; Hoffmann, M. R. iCI: iterative CI toward full CI. *J. Chem. Theory Comput.* **2016**, *12*, 1169.
- (11) Ohtsuka, Y.; Hasegawa, J.-y. Selected configuration interaction method using sampled first-order corrections to wave functions. *J. Chem. Phys.* **2017**, *147*, 34102.
- (12) Huron, B.; Malrieu, J. P.; Rancurel, P. Iterative perturbation calculations of ground and excited state energies from multiconfigurational zeroth-order wavefunctions. *J. Chem. Phys.* **1973**, *58*, 5745.
- (13) Evangelisti, S.; Daudey, J.-P.; Malrieu, J.-P. Convergence of an improved CIPSI algorithm. *Chem. Phys.* **1983**, *75*, 91.
- (14) Tubman, N. M.; Freeman, C. D.; Levine, D. S.; Hait, D.; Head-Gordon, M.; Whaley, K. B. Modern Approaches to Exact Diagonalization and Selected Configuration Interaction with the Adaptive Sampling CI Method. *J. Chem. Theory Comput.* **2020**, *16*, 2139.

- (15) Levine, D. S.; Hait, D.; Tubman, N. M.; Lehtola, S.; Whaley, K. B.; Head-Gordon, M. CASSCF with Extremely Large Active Spaces Using the Adaptive Sampling Configuration Interaction Method. *J. Chem. Theory Comput.* **2020**, *16*, 2340.
- (16) Holmes, A. A.; Tubman, N. M.; Umrigar, C. J. Heat-Bath Configuration Interaction: An Efficient Selected Configuration Interaction Algorithm Inspired by Heat-Bath Sampling. *J. Chem. Theory Comput.* **2016**, *12*, 3674.
- (17) Li, J.; Otten, M.; Holmes, A. A.; Sharma, S.; Umrigar, C. J. Fast Semistochastic Heat-Bath Configuration Interaction. *J. Chem. Phys.* **2018**, *149*, 214110.
- (18) Smith, J. E. T.; Mussard, B.; Holmes, A. A.; Sharma, S. Cheap and Near Exact CASSCF with Large Active Spaces. *J. Chem. Theory Comput.* **2017**, *13*, 5468.
- (19) Booth, G. H.; Thom, A. J. W.; Alavi, A. Fermion Monte Carlo without fixed nodes: A game of life, death, and annihilation in Slater determinant space. *J. Chem. Phys.* **2009**, *131*, 54106.
- (20) Cleland, D.; Booth, G. H.; Alavi, A. Communications: Survival of the fittest: Accelerating convergence in full configuration-interaction quantum Monte Carlo. *J. Chem. Phys.* **2010**, *132*, 41103.
- (21) Hermes, M. R.; Pandharkar, R.; Gagliardi, L. Variational Localized Active Space Self-Consistent Field Method. *J. Chem. Theory Comput.* **2020**, *16*, 4923–4937.
- (22) Liu, B.; McLean, A. A binitio potential curve for Be<sub>2</sub> ( $1\Sigma$  g+) from the interacting correlated fragments method. *J. Chem. Phys.* **1980**, *72*, 3418–3419.
- (23) Liu, B.; McLean, A. The interacting correlated fragments model for weak interactions, basis set superposition error, and the helium dimer potential. *J. Chem. Phys.* **1989**, *91*, 2348–2359.
- (24) Parker, S. M.; Seideman, T.; Ratner, M. A.; Shiozaki, T. Communication: Active-space decomposition for molecular dimers. *J. Chem. Phys.* **2013**, *139*, 021108.

- (25) Parker, S. M.; Seideman, T.; Ratner, M. A.; Shiozaki, T. Model Hamiltonian Analysis of Singlet Fission from First Principles. *J. Phys. Chem. C* **2014**, *118*, 12700–12705.
- (26) Parker, S. M.; Shiozaki, T. Quasi-diabatic States from Active Space Decomposition. *J. Chem. Theory Comput.* **2014**, *10*, 3738.
- (27) Parker, S. M.; Shiozaki, T. Communication: Active space decomposition with multiple sites: Density matrix renormalization group algorithm. *J. Chem. Phys.* **2014**, *141*, 211102.
- (28) Nishio, S.; Kurashige, Y. Rank-one basis made from matrix-product states for a low-rank approximation of molecular aggregates. *J. Chem. Phys.* **2019**, *151*, 084111.
- (29) Nishio, S.; Kurashige, Y. Importance of dynamical electron correlation in diabatic couplings of electron-exchange processes. *J. Chem. Phys.* **2022**, *156*, 114107.
- (30) Jiménez-Hoyos, C. A.; Scuseria, G. E. Cluster-based mean-field and perturbative description of strongly correlated fermion systems: Application to the one- and two-dimensional Hubbard model. *Phys. Rev. B: Condens. Matter Mater. Phys.* **2015**, *92*, 85101.
- (31) Fang, T.; Li, S. Block correlated coupled cluster theory with a complete active-space self-consistent-field reference function: The formulation and test applications for single bond breaking. *J. Chem. Phys.* **2007**, *127*, 204108.
- (32) Li, S. Block-correlated coupled cluster theory: The general formulation and its application to the antiferromagnetic Heisenberg model. *J. Chem. Phys.* **2004**, *120*, 5017–5026.
- (33) Jiménez-Hoyos, C. A.; Scuseria, G. E. Cluster-based mean-field and perturbative description of strongly correlated fermion systems: Application to the one-and two-dimensional Hubbard model. *Phys. Rev. B* **2015**, *92*, 085101.
- (34) Abraham, V.; Mayhall, N. J. Cluster many-body expansion: A many-body expansion of the electron correlation energy about a cluster mean field reference. *J. Chem. Phys.* **2021**, *155*, 054101.

- (35) Abraham, V.; Mayhall, N. J. Selected configuration interaction in a basis of cluster state tensor products. *J. Chem. Theory Comput.* **2020**, *16*, 6098–6113.
- (36) Roemelt, M.; Krewald, V.; Pantazis, D. A. Exchange coupling interactions from the density matrix renormalization group and N-electron valence perturbation theory: application to a biomimetic mixed-valence manganese complex. *J. Chem. Theory Comput.* **2018**, *14*, 166–179.
- (37) Pantazis, D. A. Meeting the challenge of magnetic coupling in a triply-bridged chromium dimer: complementary broken-symmetry density functional theory and multireference density matrix renormalization group perspectives. *J. Chem. Theory Comput.* **2019**, *15*, 938–948.
- (38) Pandharkar, R.; Hermes, M. R.; Cramer, C. J.; Truhlar, D. G.; Gagliardi, L. Localized Active Space Pair-Density Functional Theory. *J. Chem. Theory Comput.* **2021**, *17*, 2843–2851.
- (39) Pandharkar, R.; Hermes, M. R.; Cramer, C. J.; Gagliardi, L. Spin-State Ordering in Metal-Based Compounds Using the Localized Active Space Self-Consistent Field Method. *J. Phys. Chem. Lett.* **2019**, *10*, 5507–5513.
- (40) Hermes, M. R. <https://github.com/MatthewRHermes/mrh>. 2018; <https://github.com/MatthewRHermes/mrh>.
- (41) Pandharkar, R. <https://github.com/riddhish-P/mrh>. 2022; <https://github.com/riddhish-P/mrh>.
- (42) Sun, Q.; Berkelbach, T. C.; Blunt, N. S.; Booth, G. H.; Guo, S.; Li, Z.; Liu, J.; McClain, J. D.; Sayfutyarova, E. R.; Sharma, S.; Wouters, S.; Chan, G. K. L. PySCF: the Python-based simulations of chemistry framework. *WIREs Comput. Mol. Sci.* **2018**, *8*, e1340.
- (43) Robin, M. B.; Day, P. *Advances in inorganic chemistry and radiochemistry*; Elsevier, 1968; Vol. 10; pp 247–422.



- (44) Heckmann, A.; Lambert, C. Organic mixed-valence compounds: a playground for electrons and holes. *Angew. Chem., Int. Ed. Engl.* **2012**, *51*, 326–392.
- (45) D'Alessandro, D. M.; Keene, F. R. Current trends and future challenges in the experimental, theoretical and computational analysis of intervalence charge transfer (IVCT) transitions. *Chem. Soc. Rev.* **2006**, *35*, 424–440.
- (46) Brunschwig, B. S.; Creutz, C.; Sutin, N. Optical transitions of symmetrical mixed-valence systems in the Class II–III transition regime. *Chem. Soc. Rev.* **2002**, *31*, 168–184.
- (47) Joachim, C.; Gimzewski, J. K.; Aviram, A. Electronics using hybrid-molecular and mono-molecular devices. *Nature* **2000**, *408*, 541–548.
- (48) Barbara, P. F.; Meyer, T. J.; Ratner, M. A. Contemporary issues in electron transfer research. *J. Phys. Chem.* **1996**, *100*, 13148–13168.
- (49) Bao, J. J.; Zhou, C.; Varga, Z.; Kanchanakungwankul, S.; Gagliardi, L.; Truhlar, D. G. Multi-state pair-density functional theory. *Faraday Discuss.* **2020**, *224*, 348–372.
- (50) Layfield, R. A. Organometallic single-molecule magnets. *Organometallics* **2014**, *33*, 1084–1099.
- (51) Leuenberger, M. N.; Loss, D. Quantum computing in molecular magnets. *Nature* **2001**, *410*, 789–793.
- (52) Pederson, M. R.; Baruah, T. Molecular magnets: Phenomenology and theory. *Handbook of Magnetism and Advanced Magnetic Materials* **2007**,
- (53) Heisenberg, W. *Original Scientific Papers Wissenschaftliche Originalarbeiten*; Springer, 1985; pp 580–597.
- (54) Dirac, P. A. M. On the theory of quantum mechanics. *Proceedings of the Royal Society of London. Series A, Containing Papers of a Mathematical and Physical Character* **1926**, *112*, 661–677.

- (55) Van Vleck, J. H. *Electric and magnetic susceptibilities*; Clarendon Press, 1932.
- (56) Morsing, T. J.; Weihe, H.; Bendix, J. Probing Effective Hamiltonian operators by single-crystal EPR: a case study using dinuclear Cr (III) complexes. *Inorg. Chem.* **2016**, *55*, 1453–1460.
- (57) Kremer, S. EPR spectroscopic study of S= 1, 2, and 3 spin states of tris ( $\mu$ -hydroxo)-bridged chromium (III) dimers. *Inorg. Chem.* **1985**, *24*, 887–890.
- (58) Niemann, A.; Bossek, U.; Wiegardt, K.; Butzlaff, C.; Trautwein, A. X.; Nuber, B. A New Structure–Magnetism Relationship for Face-Sharing Transition-Metal Complexes with d<sup>3</sup>–d<sup>3</sup> Electronic Configuration. *Angew. Chem., Int. Ed. Engl.* **1992**, *31*, 311–313.
- (59) Bennie, S. J.; Collison, D.; McDouall, J. J. Electronic and Magnetic Properties of Kremer’s tris-Hydroxo Bridged Chromium Dimer: A Challenge for DFT. *J. Chem. Theory Comput.* **2012**, *8*, 4915–4921.
- (60) Sharma, P.; Truhlar, D. G.; Gagliardi, L. Magnetic coupling in a tris-hydroxo-bridged chromium dimer occurs through ligand mediated superexchange in conjunction with through-space coupling. *J. Am. Chem. Soc.* **2020**, *142*, 16644–16650.
- (61) Malrieu, J. P.; Caballol, R.; Calzado, C. J.; De Graaf, C.; Guihery, N. Magnetic interactions in molecules and highly correlated materials: physical content, analytical derivation, and rigorous extraction of magnetic Hamiltonians. *Chem. Rev.* **2014**, *114*, 429–492.
- (62) Neese, F. Prediction of molecular properties and molecular spectroscopy with density functional theory: From fundamental theory to exchange-coupling. *Coord. Chem. Rev.* **2009**, *253*, 526–563.
- (63) Chen, T.; Zheng, L.; Yuan, J.; An, Z.; Chen, R.; Tao, Y.; Li, H.; Xie, X.; Huang, W. Understanding the control of singlet-triplet splitting for organic exciton manipulating: a combined theoretical and experimental approach. *Scientific reports* **2015**, *5*, 1–11.

- (64) Minami, T.; Ito, S.; Nakano, M. Signature of singlet open-shell character on the optically allowed singlet excitation energy and singlet–triplet energy gap. *J. Phys. Chem. A* **2013**, *117*, 2000–2006.
- (65) Sharma, P.; Bernales, V.; Knecht, S.; Truhlar, D. G.; Gagliardi, L. Density matrix renormalization group pair-density functional theory (DMRG-PDFT): singlet–triplet gaps in polyacenes and polyacetylenes. *Chem. Sci.* **2019**, *10*, 1716–1723.
- (66) Ghosh, S.; Cramer, C. J.; Truhlar, D. G.; Gagliardi, L. Generalized-active-space pair-density functional theory: an efficient method to study large, strongly correlated, conjugated systems. *Chem. Sci.* **2017**, *8*, 2741–2750.
- (67) Nakano, M. *Excitation energies and properties of open-shell singlet molecules: applications to a new class of molecules for nonlinear optics and singlet fission*; Springer, 2014.
- (68) Anthony, J. E. Functionalized acenes and heteroacenes for organic electronics. *Chem. Rev.* **2006**, *106*, 5028–5048.
- (69) Flicker, W. M.; Mosher, O. A.; Kuppermann, A. Low energy, variable angle electron-impact excitation of 1,3,5-hexatriene. *Chem. Phys. Lett.* **1977**, *45*, 492–497.
- (70) Robinson, A. G.; Winter, P. R.; Zwier, T. S. The singlet–triplet spectroscopy of 1,3-butadiene using cavity ring-down spectroscopy. *J. Chem. Phys.* **2002**, *116*, 7918–7925.